Dynamics of electron density in a medium revealed by Mössbauer time-domain interferometry

G. V. Smirnov* and V. G. Kohn
Russian Research Center ''Kurchatov Institute,'' 123182 Moscow, Russia

W. Petry
Physik Department E-13, Technische Universität München, D-85748 Garching, Germany

(Received 16 August 1999; revised manuscript received 13 December 2000; published 23 March 2001)

Nuclear resonant scattering of synchrotron radiation allows the detection of energy transfers in the sample in the order of $\Delta E/E \approx 10^{-13}$. This extreme energy resolution is used in Mössbauer time domain interferometry to provide an inelastic scattering method similar or even superior to high resolution inelastic neutron scattering. The interferometer consists of two nuclear targets as interferometer arms, and a nonresonant sample placed in between, and detects slow dynamics of the electron density in a time range of nuclear response, typically from 10 ns to 200–500 ns. It has access to scattering vectors from 0.1 Å to beyond 10 Å. The general theory of the interferometer is provided and it is evaluated how the Van Hove correlation function presenting the electron density fluctuations of the sample in space and time can be measured. Exemplarily, it is shown how the temporal behavior of diffusion can be studied with diffusivities in the range from 10^{-16} to $10^{-13}\,m^2/s$.

DOI: 10.1103/PhysRevB.63.144303 PACS number(s): 61.10.Dp, 76.80.+y, 66.10.Cb

I. INTRODUCTION

Experiments on scattering of Mössbauer radiation by matter combine interesting features of x-ray and neutron scattering and those of Mössbauer spectroscopy. The intrinsically high energy resolution of the latter offers unique possibilities to reveal very low energy dynamics of atoms in condense media.

The electronic Rayleigh scattering of Mössbauer radiation is just like x-ray scattering with respect to the scattering mechanism and the wavelength of radiation involved. The difference lies in being able to detect by means of Mössbauer radiation very small energy changes which can occur during scattering. The energy resolution is approximately equal to the width Γ of nuclear transition ranging from 1 to 100 neV.

So to reveal such small energy transfers, the scattering experiment should employ Mössbauer radiation incident on the sample and Mössbauer absorber for the energy analysis of the scattered radiation. O'Connor and Butt[1] had applied a Mössbauer absorber just to distinguish Rayleigh recoilless and Rayleigh recoiled scattering of Mössbauer radiation with the energy transfer due to creation and annihilation of phonons. Such scattering can be treated as inelastic. For small energy transfers, in the scale of Γ, one can classify the scattering event as quasi-elastic. Only the energy changes of the order of Γ can contribute to the structure of the energy spectrum obtained with the help of Mössbauer analyzer. In this way, one can study quasi-elastic scattering associated with very soft lattice modes or spin dynamics or slow diffusive motion of atoms. In experiments on liquids, glasses, biological samples quasi-elastic line broadening was detected with the help of Rayleigh Scattering of Mössbauer Radiation called as RSMR technique; for reviews see Refs. 2 and 3.

The analog of the RSMR technique in the time domain was recently developed by Baron *et al.*[4] The scattering scheme includes two nuclear resonant targets and a nonresonant sample placed in between them. An intense pulse of synchrotron radiation (SR) passes through the system of the three scatterers and the coherently scattered radiation interferes in the detector. The two scattering channels can be distinguished when the resonance frequencies in the upstream and the downstream nuclear targets are separated. The interference of the scattering channels leads to quantum beats of the scattered intensity with time at the frequency difference. So the device works as a time domain interferometer where the wave packet scattered sequentially by the upstream resonant target and non-resonant sample is probed by the wave scattered by the downstream resonant target. In the presence of dynamics of electron density in the nonresonant sample the first wave packet can be perturbed temporally resulting in the perturbation of the interference pattern. The dynamics characterized by times of the order of the beat period and nuclear excitation lifetime can be explored by this method.

The time domain interferometry allows one to study diffusive atomic motion in materials having very different structures. To demonstrate this method, the amorphous sample of glycerol was used.[4] Besides that, as was indicated,[4] the high directionality of SR is very suitable for studying quasi-elastic scattering in the neighborhood of Bragg peaks. Quasielasticity of radiation can be found in scattering from single crystals containing fast diffusing atoms. A detailed analysis of such possibility was performed by Ruebenbauer and Wdowik[5] and recently an experiment was accomplished by Sepiol *et al.*[6]

In the present paper we develop the general theory of Mössbauer time domain interferometer in the presence of dynamics of electron density in a non-resonant sample. The time-dependent response of the sample given by the dynamical theory of diffraction is used for the first time. In particular, this allows one to study jump diffusion in crystals. Kinematical approximation of the dynamical theory equivalent to a first Born approximation is explicitly analyzed. Hence the developed theory enables analysis of scattering from the samples of arbitrary perfection and shape.

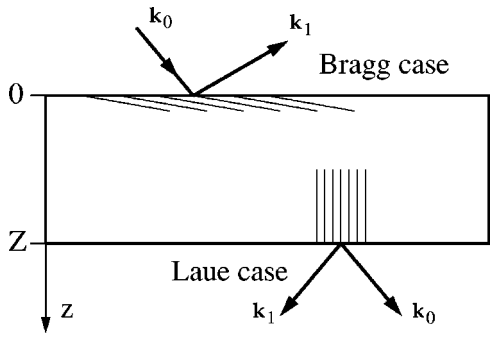

FIG. 1. Geometry of coherent scattering (Bragg diffraction) of radiation in a crystalline platelet for both Bragg and Laue cases.

Two regimes of the interferometer are considered: those in absence and in presence of radiative coupling between the arms of nuclear interferometer. Radiative coupling (RC) occurs when the delayed radiation from the upstream target is in resonance with the nuclei in the downstream target. The strongest RC takes place at zero separation of the resonances in the two nuclear targets. Throughout the paper this case will be called *RC-regime* of the interferometer. In the case of large separation of resonances, radiative coupling vanishes and one comes to a pure quantum beat solution, i.e., to a *QB-regime* of the interferometer. It corresponds to the experiment mentioned above[4].

In Sec. II the response function of the non-resonant sample is presented where *Rayleigh scattering in a dynamic system* occurs. The most complicated mathematically case of dynamical diffraction is considered. In Sec. III the principle of the Mössbauer time interferometer is considered and the time response of the two targets each having a single line resonance is analyzed for an arbitrary shift of the resonances. In Sec. IV the response of the Mössbauer time interferometer including a dynamic non-resonant sample is calculated in the QB-regime as well as in the RC regime. For the kinematical diffraction or scattering in a first Born approximation, i.e., for thin or poorly ordered sample, this response can be interpreted in terms of the intermediate scattering function in the presence of atomic motion. In Sec. V prospects of the method are considered.

II. THE RESPONSE FUNCTION OF A CRYSTALLINE SAMPLE IN TIME

In general, the Bragg diffraction in large perfect crystals is described by the dynamical theory accounting for the multiple scattering of radiation by atoms. In the dynamical theory the shape of the sample is rather significant. We consider here a crystalline sample in the form of a platelet of thickness Z (see Fig. 1). The Cartesian coordinate system is chosen so that the inward normal to the crystal entrance surface lies along the z-axis.

When the scattered wave is much less than the incident wave and the interaction of the primary radiation with atoms is only essential, the kinematical scattering is realized. The choice of the sample shape in the kinematical theory is usually the same as in the dynamical theory. The kinematical scattering may be considered as a particular case of the first Born approximation of the scattering theory when the shape of the sample appears to be not essential at all. In this section we begin with the general expressions of dynamical diffraction. The kinematical approximation is obtained then from the general formulas as a limit for a thin sample or for scattering far off Bragg angle. Finally, scattering from the systems having poor periodicity (amorphous solids and liquids) is considered.

We assume the case of the two-wave scattering (single diffracted wave) with the transmitted and diffracted waves to be linearly polarized, so that the electric polarization vectors in the waves coincide and are perpendicular to the scattering plane containing the vectors $\mathbf{k}_0$ and $\mathbf{k}_1$. We shall consider the case of reflection with change of the wave vector from $\mathbf{k}_0$ to $\mathbf{k}_1=\mathbf{k}_0+\mathbf{q}$. In the case of diffraction from the platelet, the two geometries are distinguished: Laue case, where the scattered wave emerges from the back side of the platelet, and Bragg case, where the scattered wave is at the same side of the platelet as the incident one, as is depicted in Fig. 1.

In the following we consider the response function of a crystalline sample in time. The time scale for the observation of a scattering events in the Mössbauer time domain interferometer is determined by the lifetime of the nuclear excited state and the characteristic time of the dynamics of the electron density. Both exceed tremendously the period of the carrier oscillation of the electromagnetic field. Because of the weak interaction of the radiation field with the atoms in the target, the characteristic length of the interaction much exceeds the radiation wavelength. These two properties allow us to perfectly separate the fast space-time oscillations of the field strength from the slow variation of their envelopes in time and space.

The diffraction from the electronic sub-system of the crystal occurs promptly at the instant state of the electron density distribution. In a dynamical scattering system the electron density distribution is varying in time. Therefore, the electronic susceptibility of the system and the scattering amplitude turn out to be time dependent.

The time response of the sample $G_S(\mathbf{q},t-t')$ to the short pulse of radiation (in the considered time scale) can be expressed in terms of the field envelopes. In both Bragg and Laue cases we have $G_S(\mathbf{q},t-t')=\delta(t-t')g_S(\mathbf{q},t)$, where $\delta(t-t')$ is the Dirac delta function, and $g_S(\mathbf{q},t)=\sqrt{\gamma_1/\gamma_0}E_1(Z,t)/E_0(0,t)$ in the Laue case and $g_S(\mathbf{q},t)=\sqrt{\gamma_1/\gamma_0}E_1(0,t)/E_0(0,t)$ in the Bragg case, where $\gamma_{0,1}=k_{0z,1z}/K$ (with $k_{0z,1z}$ being projections of $\mathbf{k}_{0,1}$ on the z-axis); magnitude $\gamma_1<0$ for Bragg case and $\gamma_1>0$ for Laue case.

The dynamical theory is well presented in the literature (see, for example, Ref. 7); therefore, we write down only the final expressions for $g_S(\mathbf{q},t)$ in a compact and symmetric form. In the Laue case,

$$g_S(\mathbf{q},t)=B_1B_2\frac{X_1-X_2}{B_1-B_2}; \tag{1}$$

and in the Bragg case,

$$g_S(\mathbf{q},t)=B_1B_2\frac{X_1-X_2}{B_1X_1-B_2X_2}. \tag{2}$$

Here the following notations are used

$$X_{1,2}=\exp\left\{ i\frac{KZ}{2\gamma_0}[\chi_0+\chi_q^-\beta^{1/2}B_{1,2}]\right\},$$

$$B_1=-\frac{\beta^{1/2}\chi_q}{A+\sqrt{A^2+\beta\chi_q\chi_q^-}},$$

$$B_2=-\frac{\chi_q}{\chi_q^-B_1},\quad A=-\frac{1}{2}\left(\alpha_q\beta+\chi_0\frac{1-\beta}{\beta}\right),$$

$$\alpha_q=\frac{(\mathbf{k}_q^2-K^2)}{K^2},\quad \beta=\frac{\gamma_0}{\gamma_1}. \tag{3}$$

In Eq. (3) the square root has positive imaginary part. The parameters χ_q represent the Fourier coefficients in the expansion of the electronic susceptibility in q-space. These Fourier coefficients are time dependent functions due to fluctuations of the electron density. Obviously, the fluctuations do not change the average electron density in the sample. Therefore, both the scattering amplitude in the forward direction and the susceptibility coefficient χ_0 do not depend on time.

We note that in crystals the electron density is a spatially periodic function; therefore, the susceptibility coefficients can be calculated by integration over the crystalline unit cell. Nevertheless, for generality, we assume them to be integrated (averaged) over the volume exceeding essentially the unit cell volume that allows us to consider irregular systems as well.

In a thin single crystal, as well as in a system having poor periodicity where the coherent scattering amplitude is small, i.e., when the condition is fulfilled $KZ|\chi_q|\ll 1$, the kinematical approximation of the dynamical theory works fairly well. In general, the kinematical approximation is valid when the amplitude of the scattered wave is much less than that of the incident wave. Then the response function is reduced to an especially simple form

$$g_S(\mathbf{q},t)=\pm i\chi_q(t)\frac{KZ}{2\sqrt{\gamma_0\gamma_1}}\exp\left(i\frac{KZ}{2\gamma_0}\chi_0\frac{(1\pm 1)}{2}\right)$$
$$=CR(\mathbf{q},t), \tag{4}$$

where the upper/lower sign refers to Laue/Bragg case. The formula (4) becomes valid for the sample of arbitrary shape and for q being not only the reciprocal lattice vector when the factor C is taken in an appropriate way.

Note, that in all cases of applicability the Eq. (4) the response function is proportional to the Fourier coefficient of electron density $R(\mathbf{q},t)$, which is the only factor determining the time dependence of the sample response. For the dynamical diffraction this is not the case. The time dependence of the sample response has a much more complicated form.

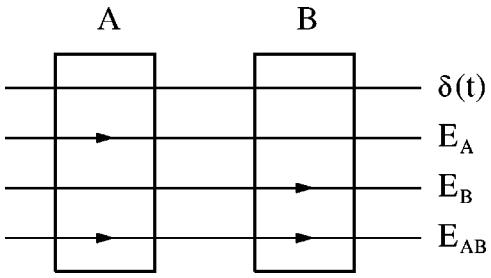

FIG. 2. Schematic presentation of the four scattering channels of a SR pulse through two subsequent nuclear resonant targets. Arrows symbolize quantum absorption events.

III. MÖSSBAUER TIME DOMAIN INTERFEROMETRY USING SYNCHROTRON RADIATION

Let the SR pulse be passing through a system of spatially separated scatterers. We assume an external perturbation applied to a scatterer to be homogeneous in time. As it was shown in Ref. 8 (see also Ref. 9), the time response of such a system to a $\delta(t)$-function excitation can be presented by a convolution of the time responses of individual scatterers. We consider a system consisting of two nuclear resonant scatterers A and B, see Fig. 2. The time response of such a system can be found as convolution of the responses of targets A and B

$$G_{AB}(t)=\int_{-\infty}^{+\infty}dt'G_B(t-t')G_A(t'). \tag{5}$$

The response functions $G_A(t)$ and $G_B(t)$ in the case of nuclear forward scattering of SR from a target having single line structure of its resonance is given in Ref. 8. In the case of resonance broadening, with the line preserving a Lorentzian shape (e.g., the case of free diffusion in a liquid), the response function of a single target is as follows (see, e.g., Refs. 10 and 11)

$$G(t)=\exp(-\mu_e z_0/2)\exp(-i\omega_r t)$$
$$\times\left\{\delta(t)-\theta(t)\frac{T}{2t_n}\exp(-q\tau/2)\,\sigma(T\tau)\right\}, \tag{6}$$

where ω_r is the resonance frequency; $\tau=t/t_n$, $t_n=\hbar/\Gamma$ is the lifetime of the excited nuclear state; $T=\mu_r z_0$, μ_r and μ_e are nuclear resonance and electronic absorption coefficients; z_0 is the thickness of nuclear scatterer; $\sigma(T\tau)=J_1(\sqrt{T\tau})/\sqrt{T\tau}$ with $J_1(x)$ being a Bessel function of the first order; $\theta(t)$ is a Heaviside step function equal to zero at negative arguments. Here we use symbol q for the dimensionless parameter of resonance broadening to be consistent with the previous works,[10–12] $q\geqslant 1$. Do not confuse it with modulus of the scattering vector $\mathbf{q}$.

As seen from Eq. (6), the response function contains both the prompt and the delayed parts. The delayed part has a carrier frequency coinciding with that of the nuclear resonance. If targets A and B are identical (in material and thickness) and the resonance frequency in the first target is Doppler shifted with respect to that in the second target by a

value Ω, then the total time response obtained after substitution of Eq. (6) into Eq. (5) is as follows:

$$G_{AB}(t)=\exp(-\mu_e z_0)\Big[\delta(t)-\exp(-i\omega_r t)\times\Big\{\psi(t)\exp(-i\Omega t)+\psi(t)-\int_0^t dt'\,\psi(t-t')\psi(t')\exp(-i\Omega t')\Big\}\Big], \quad (7)$$

where the following function is introduced:

$$\psi(t)=\frac{T}{2t_n}\exp(-q\tau/2)\sigma(T\tau). \quad (8)$$

The terms containing $\psi(t)$ in Eq. (7) represent the delayed γ ray emission (for the time $t>0$).

Equation (7) is the response function of the system containing the two resonant targets (see Ref. 13). As seen from Eq. (7), the scattering event can be represented by superposition of the four scattering channels (see also Fig. 2): transmission of the SR pulse without interaction with nuclei, given by $\exp(-\mu_e z_0)\delta(t)$; nuclear resonance scattering of the SR by the upstream target, given by the first term of the delayed part, E_A; nuclear resonance scattering of the SR by the downstream target, given by the second term of the delayed part, E_B; and double nuclear resonance scattering of the SR first by the upstream and then by downstream target, presented by the last integral term of the delayed part, E_{AB}. This last term actually presents the radiative coupling of the nuclear currents in the upstream target with those in the downstream target via the coherent field propagating in the forward direction. *Thus the response of the system is determined by the sum of responses of the constituent parts and of the term presenting the radiative coupling of the parts.*

When $\Omega \gg \Gamma/\hbar$ then the integral in Eq. (7) representing the radiative coupling of the two targets is small, and can be neglected. So the time dependence of the delayed intensity takes a simple form

$$I_{AB}=|G_{AB}(t)|^2 \approx 2Y(t)[1+\cos(\Omega t)] \quad (9)$$

with $Y(t)=\exp(-2\mu_e z_0)\psi^2(t)$. The interference of the two scattering channels, presented by the second and third terms in Eq. (7), yields a quantum beat pattern of the scattering intensity given by Eq. (9). In the case of small electronic absorption the intensity averaged over the quantum beat period turns out to be twice as large as the intensity scattered by an individual target. Thus, in the averaged intensity, the two targets behave as independent scatterers. When Ω becomes comparable with $\Gamma/\hbar$ the targets can no longer be considered as independent scatterers (see Sec. IV B).

The time structure of the quantum beating can be compared with the Moire pattern arising due to interference of light coming from two spatially separated coherent sources. In our case, each target behaves as an independent coherent emitter. It is well known that Moire patterns are highly sensitive to very little changes of the radiation phase, when a phase shifter is inserted into one of the interfering beams. Obviously, the time domain interference should be also very sensitive to a phase and amplitude change due to scattering from a non-resonant sample placed in between two resonant targets, which can be regarded as the arms of an interferometer.

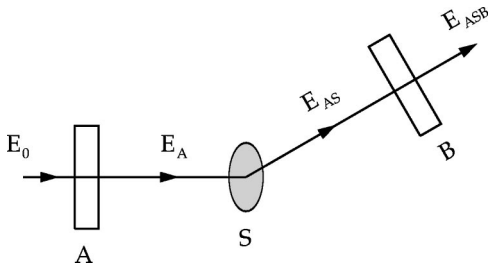

FIG. 3. Scheme of a Mössbauer time domain interferometer. *A* and *B*: resonant targets; S: a nonresonant sample. E_A, E_{AS}, and E_{ASB} present transformation of the field strength in passage of radiation through the system.

This fact was convincingly demonstrated in Ref. 4, where the sample of glycerol was placed between the two Mössbauer scatterers and the measurements of the beat patterns were performed at different temperatures of glycerol. In this compound the electron density appears to be time dependent within the nuclear lifetime window and this results in the time dependent perturbation of the amplitude and phase of the scattered radiation. We consider the scattering from such a system in the next section.

IV. IMPACT OF RAYLEIGH SCATTERING ON THE INTERFERENCE PATTERN

Let us now contemplate the system of three subsequent scatterers depicted in Fig. 3. Between the two nuclear resonant targets *A* and *B*, which are the arms of the interferometer, a non-resonant electronic scatterer, target *S*, is placed as a sample. The radiation wave packet is transformed in passage through the system, as shown in Fig. 3. The nuclear forward scattering of SR pulse occurs in target *A* and the wave packet E_A is formed. It contains the prompt and delayed part, as described by Eq. (6). This wave packet is incident on a diffusive target *S*, where electronic coherent scattering characterized by a scattering vector **q** takes place. At this stage, the E_A wave packet is transformed into the E_{AS} wave packet that can be modulated due to a possible dynamics of the electronic density in the sample. Finally, the E_{AS} wave packet is scattered in the new forward direction by nuclei in target *B*, which works as an analyzer of the radiation scattered by sample, i.e., of the E_{AS} wave packet.

The scattering in the sample is prompt by its nature, in contrast to that in a resonant target. Since the flight time through the system can be neglected, the scattering in the sample occurs at the moment when radiation emerges from target *A*. So the response functions of target *A* and sample *S* contain the same time argument, and the combined response function of the two targets is simply the product of functions $G_A(t)$ and $g_S(t)$.

Therefore, the response function of the entire system can be found using the relation similar to that given by Eq. (5)

$$G_{ASB}(t)=\int_{-\infty}^{+\infty} dt' G_B(t-t') g_S(\mathbf{q},t') G_A(t'), \quad (10)$$

where t' is the emission time from target *A*, the scattering time from target *S* and the excitation time of target *B*; t is the deexcitation time of target *B*. The time zero is set by the arrival of the SR pulse at the detector.

Comparing Eqs. (10) and (5), we see that the response of the scattering system can be decomposed again into the four parts presenting the scattering channels through the resonant targets (see the previous section). However, the wave packets formed in each channel are now perturbed by the scattering in the sample due to a possible dynamics of the electronic density. We analyze effect of the perturbation separately for the two different regimes of the interferometer.

A. Quantum beat regime of the interferometer

Applying Eq. (6) to Eq. (10) and assuming a large difference of resonance frequencies Ω, we obtain for the delayed part of the response function

$$G_{ASB}(t)=-\exp(-\mu_e z_0) g_S(\mathbf{q},t)\exp(-i(\omega_r+\Omega)t)\psi(t) - \exp(-\mu_e z_0) g_S(\mathbf{q},0)\exp(-i\omega_r t)\psi(t). \quad (11)$$

As seen, in this case, the response of the system is determined by the interference of two scattering channels. In the first channel the delayed part of radiation emerging from target *A* is electronically scattered in sample *S* at time *t*. In the second channel the prompt part of radiation emerging from target *A* is first electronically scattered in the sample at time 0, immediately absorbed by nuclei in target *B* and then reemitted in the form of delayed nuclear radiation at time *t*.

The carrier frequencies of the scattered waves are shifted by Ω. Therefore, the interference of the waves yields a QB-pattern at frequency Ω. However, the interference pattern is perturbed by a stochastic variation of the response function of the non-resonant sample, $g_S(\mathbf{q},t)$. The time dependence of this response function is provided by the dynamics of the electron density in the sample. Just this stochastic variation of the sample response breaks partly (to lesser or larger extent depending on the internal dynamics in the sample) the phase correlation between the interfering waves and leads, in general, to an attenuation of the interference contrast with time.

Now we find the time dependence for the scattering intensity at $t>0$

$$I_{ASB}(t)=|G_{ASB}(t)|^2=Y(t)[|g_S(\mathbf{q},t)|^2+|g_S(\mathbf{q},0)|^2 + 2|g_S(\mathbf{q},t)g_S(\mathbf{q},0)|\cos(\Omega t+\varphi_S(0)-\varphi_S(t))], \quad (12)$$

where $\varphi_S(t)$ is the phase of the complex function $g_S(\mathbf{q},t)$.

In the limit of a weak scattered wave in accord with Eq. (4), the function $g_S(\mathbf{q},t)$ is proportional to the spatial Fourier transform of the electron density $\rho(\mathbf{r},t)$

$$R(\mathbf{q},t)=\int d\mathbf{r}\rho(\mathbf{r},t)\exp(-i\mathbf{qr}). \quad (13)$$

Expression (12) represents the time dependence of the delayed scattering intensity following a particular SR pulse. It includes the time dependent response of the non-resonant target. Since the dynamics of the electron density in the sample is not correlated with the arrival of the SR pulses, the measured intensity is obtained as a result of averaging of a single scattering event over many SR passages. The averaging of expression (12) is, in fact, adding of independent QB-patterns perturbed stochastically due to dynamics of electron density.

1. Averaging in the case of weak scattering

As mentioned above, the Fourier transform of the electron density [see Eq. (13)] can be used to find the intensity of weak scattering. Therefore, in the expression for the intensity Eq. (12), the function $g_S(\mathbf{q},t)g_S(\mathbf{q},t')$ can be written in terms of electron density $C^2\int d\mathbf{r}\,d\mathbf{r}'\exp[-i\mathbf{q}(\mathbf{r}-\mathbf{r}')]\rho(\mathbf{r},t)\rho(\mathbf{r}',t')$. Under the conditions of the thermodynamic equilibrium the correlations referring to particular times are identical and depend only on the scattering vector $\mathbf{q}$. They are determined by geometrical arrangement of the mean position of atoms (structure factors) and by the average spatial distribution of atoms around their mean positions (Debye Waller factors). Therefore, to get the observed intensity, one has to calculate only the correlator containing different times [third term in Eq. (12)]. The result is expressed via the intermediate scattering function which is the time Fourier transform of the dynamic structure factor of the sample

$$S(\mathbf{q},t-t')=\int d\mathbf{r}\,d\mathbf{r}'\exp[-i\mathbf{q}(\mathbf{r}-\mathbf{r}')]\langle\rho(\mathbf{r},t)\rho(\mathbf{r}',t')\rangle. \quad (14)$$

Here $\langle\cdots\rangle$ means averaging over the time of passage of SR pulses.

If we suppose the correlator to be a real function—which is most frequently the case—then we arrive at the formula for the averaged intensity analogous to that used for interpretation of the experimental results in Ref. 4,

$$\overline{I}_{ASB}(t)\approx 2Y(t)C^2[S(\mathbf{q},0)+S(\mathbf{q},t)\cos(\Omega t)]. \quad (15)$$

2. Intermediate scattering function in the presence of atomic diffusion

In a solid state medium a Fourier coefficient of the electron density can be presented as follows:

$$R(\mathbf{q},t)=\sum_a \exp\{-i\mathbf{q}[\mathbf{r}_a+\mathbf{u}_a(t)]\}f_a(\mathbf{q})\exp[-W_a(\mathbf{q})/2], \quad (16)$$

where $\mathbf{r}_a$ is the mean value of the coordinate of the ath atom; $f_a(\mathbf{q})$ is the atomic structure factor equal to the Fourier coefficient of the electron density of an atom; $\exp[-W_a(\mathbf{q})/2]$ is a square root of the Debye-Waller factor that is obtained

while averaging over the fast thermal oscillations of atoms. Finally, $\mathbf{u}_a(t)$ is the displacement of an atom due to diffusive motion of which the average velocity is small and leads to a little displacement (of the order of the wavelength of radiation) during the lifetime of the nuclear excited state.

Introducing a specific time t_0 of the SR pulse passage through the interferometer and performing averaging over t_0, we obtain for the intermediate scattering function [compare with Eq. (14)]

$$S(\mathbf{q},t)=\frac{1}{t_m}\int dt_0 R(\mathbf{q},t_0+t)R^*(\mathbf{q},t_0), \tag{17}$$

where t_m is the full measurement time including macroscopic number of SR pulses. The integration is performed over this full time. The expression for the Fourier coefficient of the electronic density Eq. (16) can be re-written in the form where the time independent term is isolated

$$R(\mathbf{q},t)=\sum_a A_a(\mathbf{q})\exp(-i\mathbf{q}\mathbf{r}_a) - 2i\sum_a A_a(\mathbf{q})\exp(-i\mathbf{q}[\mathbf{r}_a+\mathbf{u}_a(t)/2]) \times\sin[\mathbf{q}\mathbf{u}_a(t)/2] \tag{18}$$

with $A_a(\mathbf{q})=f_a(\mathbf{q})\exp[-W_a(\mathbf{q})/2]$. In this presentation the Fourier coefficient is the sum of the static and dynamic contributions

$$R(\mathbf{q},t)=\overline{R}(\mathbf{q})+\delta R(\mathbf{q},t). \tag{19}$$

Substituting Eq. (18) into Eq. (17), we obtain for the intermediate scattering function the following expression:

$$S(\mathbf{q},t)=|\overline{R}(\mathbf{q})|^2+\frac{1}{t_m}\int dt_0\,\delta R(\mathbf{q},t_0+t)\,\delta R^*(\mathbf{q},t_0). \tag{20}$$

The static term in the intermediate scattering function presents the elastic scattering of radiation by the time averaged crystalline lattice, whereas the dynamic term presents the quasielastic scattering caused by diffusion of atoms in a crystal. For the elastic contribution we have

$$|\overline{R}(\mathbf{q})|^2=\sum_a\sum_b A_a(\mathbf{q})A_b(\mathbf{q})\exp(-i\mathbf{q}[\mathbf{r}_a-\mathbf{r}_b]). \tag{21}$$

If a long range correlation in the atomic positions takes place the Bragg scattering can happen. The intensity in Bragg direction is proportional to N^2, where N is number of atoms in the unit volume. In the other limit case, i.e., in the absence of atomic order, the scattering intensity is proportional to N. Thus the ratio between the elastic and quasielastic scattering intensities is determined to a great extent by regularity of the scattering system. In the case of perfect crystals, the elastic contribution into the intermediate scattering function dominates at the Bragg angle. Since in this case the intermediate scattering function $S(\mathbf{q},t)$ is nearly time independent, one cannot observe practically the decay of QB pattern described by Eq. (15) and hence cannot see any effect of diffusion. Recently such a result was obtain experimentally by authors of Ref. 6. However, the elastic scattering contribution can be essentially weakened by shifting the crystal off a Bragg reflection far at its wings. Therein one can find the effect of diffusive motion of atoms.

In the poorly ordered systems, like glassy and amorphous materials, the role of elastic scattering is largely decreased. Combining Eqs. (16) and (17), we obtain the following expression for the intermediate scattering function:

$$S(\mathbf{q},t)=\sum_a\sum_b A_a(\mathbf{q})A_b(\mathbf{q})\exp[-i\mathbf{q}(\mathbf{r}_a-\mathbf{r}_b)] \times\frac{1}{t_m}\int dt_0\exp\{-i\mathbf{q}[\mathbf{u}_a(t_0+t)-\mathbf{u}_b(t_0)]\}. \tag{22}$$

Assuming the non-correlated motion of different atoms (like in an amorphous or glassy sample), we obtain for $\mathbf{q}$ not equal to zero all terms with $a\neq b$ to be randomly phased and thus canceling each other in average. Consequently, in the random phase approximation, we may neglect the contribution from these terms. Furthermore, we take into account that the scattering system may consist of atoms of different kinds. Then the atomic index a has to be replaced by two indices a, j, where index a indicates now the sort of atom and index j numbers the atoms of a given type. Equation (22) has to be replaced approximately by

$$S(\mathbf{q},t)=\sum_a A_a^2(\mathbf{q})\frac{1}{t_m}\int dt_0 \times\sum_j \exp\{-i\mathbf{q}[\mathbf{u}_{aj}(t+t_0)-\mathbf{u}_{aj}(t_0)]\}. \tag{23}$$

The sum over j in the right-hand part of this expression was analyzed in Ref. 10, where it was shown to be proportional to the single particle Van Hove function $F_{sa}(\mathbf{q},t)$ and does not depend on time t_0. Hence we obtain the expression

$$S(\mathbf{q},t)=\sum_a N_a A_a^2(\mathbf{q})F_{sa}(\mathbf{q},t), \tag{24}$$

where N_a is the number of atoms of the sort a in the unit volume of the scattering media. The scattering in this case is entirely quasielastic, and its intensity is proportional to the number of atom in the unit volume. The Van Hove function $F_{sa}(\mathbf{q},t)$ was investigated in detail in the original work,[14] as well as in Refs. 10, 12 and 15.

Since $F_{sa}(\mathbf{q},t)$ is a decaying function of time, one can deduce from Eqs. (15) and (24) that the main effect caused by diffusion of atoms in a non-resonant sample is a reduction with time of the quantum beat amplitude in the transmitted intensity.

Figure 4 illustrates the impact of diffusion in the QB-regime of the Mössbauer time domain interferometer. The interferometer arms are supposed to be 1 μm SS foils enriched by ^{57}Fe up to 95%. It is assumed that the intermediate scattering function decays exponentially (like in the case of

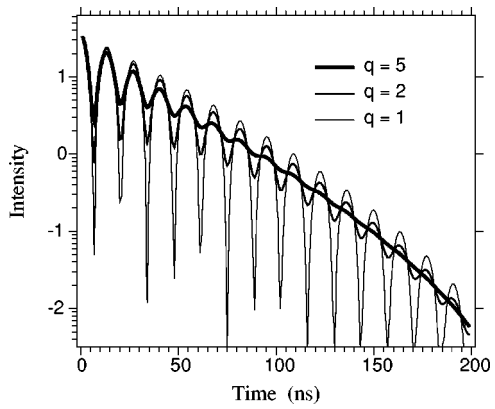

FIG. 4. Diffusion in a non-resonant sample revealed in quantum beat regime of the interferometer for different diffusion rates, $q=1$ corresponds to absence of diffusion.

free diffusion where the resonance broadening is given by the parameter $q=1+2DK^2t_n$ with D as a diffusion coefficient) $F_s(t)=\exp(-(q-1)\tau)$ having $q=1,2,5,\ \tau=t/t_n$. It is well seen that the contrast in QB pattern decreases quite rapidly with the diffusion rate. Already at $q=5$ corresponding to a diffusion coefficient $D\approx 10^{-14}\,\mathrm{m}^2/\mathrm{s}$, quantum beats are observed only in the initial stage of the decay. Thus the QB-regime of the Mössbauer interferometer is highly sensitive to diffusion in the range $10^{-16}<D<10^{-14}\,\mathrm{m}^2/\mathrm{s}$. The possibility of such experiments was demonstrated in Ref. 4.

The essential difference between Rayleigh electronic and resonant nuclear scatterers is that in the former case the Van Hove function arises only at non-zero scattering vector $\mathbf{q}$, while in the latter it may exist in the forward scattering.[10] In the case of forward scattering from the non-resonant sample, the Van Hove function equals unity, so that the diffusive non-resonant scatterer makes no impact on the time evolution of the forward scattered intensity.

3. General correlation function

Obviously, the expression for scattering intensity in general case Eq. (12) should be also averaged over time t_0 of the SR pulse passage through the interferometer. Performing averaging over t_0, one has for the averaged intensity

$$\overline{I}_{ASB}(t)\approx Y(t)\frac{1}{t_m}\int dt_0[|g_S(\mathbf{q},t_0+t)|^2+|g_S(\mathbf{q},t_0)|^2 + 2|g_S(\mathbf{q},t_0+t)g_S(\mathbf{q},t_0)| \times\cos(\Omega t+\varphi_S(t_0)-\varphi_S(t_0+t))]. \tag{25}$$

The result of integration can be expressed in terms of a real function

$$B(\mathbf{q},t)=\frac{1}{t_m}\int dt_0 g_S(\mathbf{q},t_0+t)g_S^*(\mathbf{q},t_0) \tag{26}$$

which will be called *the general correlation function*. Finally, in analogy with Eq. (15), we arrive at the expression in the general case

$$\overline{I}_{ASB}(t)\approx 2Y(t)[B(\mathbf{q},0)+B(\mathbf{q},t)\cos(\Omega t)]. \tag{27}$$

We find now the approximate expression for the general correlation function in the case where the atomic dynamics has a character of small perturbation. The response of the sample $g_S(\mathbf{q},t)$ can be splitted into static and dynamic parts as well. If the dynamic correction to the electron density is small (as supposed) compared to the time averaged density, one can use the following approximate expression for $g_S(\mathbf{q},t)$:

$$g_s(\mathbf{q},t)=\overline{g_s}(\mathbf{q})+D_s(\mathbf{q})\,\delta R(\mathbf{q},t),\quad D_s(\mathbf{q})=\frac{\partial g_s(\mathbf{q},t)}{\partial R(\mathbf{q})}. \tag{28}$$

We substitute this expansion into Eq. (26) and obtain

$$B(\mathbf{q},t)=|\overline{g_s}(\mathbf{q})|^2+|D_s(\mathbf{q})|^2 \times\frac{1}{t_m}\int dt_0\,\delta R(\mathbf{q},t_0+t)\,\delta R^*(\mathbf{q},t_0). \tag{29}$$

The integrals of type $\overline{g_s}(\mathbf{q})D_s^*(\mathbf{q})\int dt_0\,\delta R^*(\mathbf{q},t_0)$ containing the first power of $\delta R(\mathbf{q},t)$ does not contribute because the average value of the time dependent correction to the electron density equals zero. The static part of the general correlation function $|\overline{g_s}(\mathbf{q})|^2$ again is dominant in the presence of a strong Bragg scattering. As a result, the quantum beat visibility in Eq. (27) remains almost unchanged with time. The diffusive motion of atoms can hardly be observed under these conditions.

B. Electron density dynamics observed in radiative coupling regime

Now we consider the performance of the interferometer under conditions of very little or zero shift of the resonances in the interferometer arms $\Omega\leqslant\Gamma/\hbar$. In this case, the radiative coupling between the resonant parts of the scattering system plays a significant role. Obviously, the perturbation of the upstream wave packet, $E_A\Rightarrow E_{AS}$ (see Fig. 3), due to quasi-elastic scattering in the sample will effect the radiative coupling between the interferometer arms. This effect can be revealed in the time dependence of the scattering intensity.

While calculating the response of the system in accord with Eq. (10), one can no longer neglect the channel where the double resonance scattering of SR pulse first in target A and then in target B takes place.

The calculation of the response function given by Eq. (10), with the account for the radiative coupling, leads to the following expression:

$$G_{ASB}(t)=\exp(-\mu_e z_0)\exp(-i\omega_r t)\Big\{g_S(\mathbf{q},0)\,\delta(t) - g_S(\mathbf{q},t)\exp(-i\Omega t)\,\psi(t)-g_S(\mathbf{q},0)\,\psi(t) + \int_0^t dt' g_S(\mathbf{q},t')\,\psi(t-t')\exp(-i\Omega t')\,\psi(t')\Big\}. \tag{30}$$

This is the *response function of the interferometer including a sample with an account for the radiative coupling between the resonant targets*. The four scattering channels are open now and in all four channels the interaction with the sample is involved. The first channel presents transmission of the SR pulse through the system without interaction with nuclear targets. The next two channels are the same acting in QB-regime of the interferometer; see Eq. (11). The last channel is specific for the present case. It presents sequential scattering of radiation by all three elements of the system. Here the convolution with the response of the sample at running time t' is performed. In general, we see that the dynamics of electron density in the sample reveals itself in RC-regime in a more complicated way.

The delayed scattering intensity takes the following form [we assume in our calculation the function $\psi(t)$ [see Eq. (8)] to be real]

$$
\begin{aligned}
I_{ASB}(t) = Y(t)\{&|g_S(\mathbf{q},t)|^2 + |g_S(\mathbf{q},0)|^2 \\
&+ 2\,\mathrm{Re}[g_S(\mathbf{q},t) g_S^*(\mathbf{q},0)\exp(-i\Omega t)]\} \\
&- 2M\,\mathrm{Re}\Big\{ \psi(t)[g_S^*(\mathbf{q},t)\exp(i\Omega t) + g_S^*(\mathbf{q},0)] \\
&\times \int_0^t dt'\,\psi(t-t') g_S(\mathbf{q},t')\,\psi(t')\exp(-i\Omega t') \Big\} \\
&+ M\left| \int_0^t dt'\,\psi(t-t') g_S(\mathbf{q},t')\,\psi(t')\exp(-i\Omega t') \right|^2 ,
\end{aligned}
\tag{31}
$$

where $M = \exp(-2\mu_e z_0)$. This expression has to be averaged over many SR passages. While doing this, only the product of the response functions of the non-resonant sample referring to different times has to be averaged. The result of averaging can be expressed again via the function $B(\mathbf{q},t)$ determined by Eq. (26). Performing the change of variables $t' \Rightarrow t - t'$, where it is necessary we arrive to the following result:

$$
\begin{aligned}
\overline{I}_{ASB}(t) = 2Y(t)&[B(\mathbf{q},0) + B(\mathbf{q},t)\cos(\Omega t)] \\
&- 4M\psi(t)\int_0^t dt'\,\psi(t-t') B(\mathbf{q},t')\,\psi(t')\cos(\Omega t') \\
&+ M\int_0^t dt' \int_0^{t'} dt''\,\psi(t-t')\,\psi(t') B(\mathbf{q},t'-t'') \\
&\times \psi(t-t'')\,\psi(t'')\cos[\Omega(t'-t'')].
\end{aligned}
\tag{32}
$$

In the case where the two resonant targets have coincident resonances, $\Omega = 0$, Eq. (32) takes the form

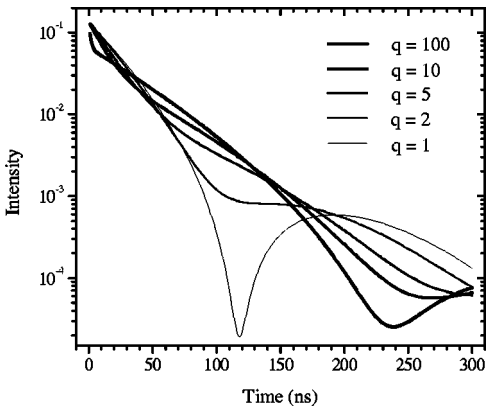

FIG. 5. Diffusion in a non-resonant sample as seen in the radiative coupling regime of the interferometer. The lines of increasing thicknesses correspond to different q.

$$
\begin{aligned}
\overline{I}_{ASB}(t) = 2Y(t)&[B(\mathbf{q},0) + B(\mathbf{q},t)] \\
&- 4M\psi(t)\int_0^t dt'\,\psi(t-t') B(\mathbf{q},t')\,\psi(t') \\
&+ 2M\int_0^t dt' \int_0^{t'} dt''\,\psi(t-t')\,\psi(t') B(\mathbf{q},t'-t'') \\
&\times \psi(t-t'')\,\psi(t'').
\end{aligned}
\tag{33}
$$

Although the quantum beats are absent in this case, the time evolution of the scattering intensity appears to be strongly dependent on the general correlation function $B(\mathbf{q},t)$.

In the limit of weak scattering the function $B(\mathbf{q},t)$ is simply proportional to the intermediate scattering function, which in turn, in the case of random phase approximation, is proportional to the Van Hove function $F_s(\mathbf{q},t)$ (we assume here system consisting of one sort of atoms). In the RC-regime, this function influences the time dependence of the scattering intensity not in that simple fashion as in QB-regime; compare Eqs. (33) and (15) [with $B(\mathbf{q},t)$ and $S(\mathbf{q},t)$ replaced by $F_s(\mathbf{q},t)$].

Figure 5 shows an example of the time evolution at different diffusion rates. For illustration we have used the model of free diffusion, where the spectral density of the self-correlation function is described by a Lorentzian distribution having the broadening parameter q. As interferometer arms, ^{57}Fe enriched SS foils of 1 μm thickness are used. The sensitivity of the time dependences to the diffusive motion of atoms in the sample is evident. The perturbation of the upstream wave packet due to quasi-elastic scattering in the sample disrupts the radiative coupling between the nuclear targets, which is revealed in a change of speed-up of the γ ray emission and in a change of its dynamical beating (for general properties of nuclear forward scattering see, e.g., Ref. 13). Namely, the diffusion causes the acceleration of γ ray emission at the first stage, deacceleration of the emission at a later stage, and a shift of the dynamical beating.

While the QB-regime is sensitive to diffusion in the range of resonance broadening $1 < q < 5$, the RC-regime is sensi-

tive to diffusion in a broader range $1<q<100$. Thus it essentially extends the sensitivity of the method to higher diffusion rates.

V. SUMMARY

The general theory of synchrotron radiation (SR) scattering in the Mössbauer time domain interferometer in the presence of dynamics of electron density in a non-resonant sample is developed. The interferometer is a scattering system where the wave packet of SR scattered sequentially by the upstream resonant target and non-resonant sample is analyzed by the downstream resonant target. The two resonant targets can be regarded as the arms of the interferometer. In the presence of dynamics of electron density in the non-resonant sample, the wave packet arriving at the analyzer is temporally perturbed resulting in the perturbation of the interference pattern. Electron density dynamics can be explored by this method in the scale of the nuclear excitation lifetime.

Two regimes of the interferometer are analyzed: those in absence and in presence of radiative coupling between the arms of nuclear interferometer. These regimes are realized at a large and zero separation of resonances in the arms, the quantum beat regime, and radiative coupling regime, respectively.

The scattering intensity is expressed in terms of the response function of the resonant targets and the general correlation function. In the limit of weak scattering (scattering at the wings of Bragg reflection far off Bragg angle, or from a thin sample or a poorly ordered sample), the general correlation function is simply proportional to the intermediate scattering function of the sample, which in the case of random phase approximation, is proportional to the Van Hove function $F_s(\mathbf{q},t)$.

The essential difference between Rayleigh electronic and resonant nuclear scatterers is that in the former case, the Van Hove function arises only at non-zero scattering vector $\mathbf{q}$, while in the latter it may exist in the forward scattering.[10] In the case of forward scattering from the non-resonant sample the Van Hove function equals unity, so that the diffusive non-resonant scatterer makes no impact on the time evolution of the forward scattered intensity.

One is able to present the general correlation function as the sum of static and dynamics contributions. The static one represents the Rayleigh scattering from the time averaged crystalline lattice, while the dynamic one represents the quasielastic scattering from the time variable electron density. In presence of a strong Bragg scattering, the static part dominates and makes the observation of atomic dynamics by means of the time domain interferometry almost impossible. The either way to diminish the elastic channel of scattering (going far off Bragg angle in case of perfect crystals, using thin samples, or poorly ordered samples like, e.g., glassy material) will help to extract and investigate the atomic diffusion motion.

Since general correlation function and intermediate scattering function are decaying functions of time, the main effect caused by the diffusion of atoms in a non-resonant sample in a QB-regime is a reduction with time of the quantum beat visibility in the interference pattern. The QB-regime of the Mössbauer interferometer is sensitive to diffusion in the range $10^{-16}<D<10^{-14}\,\mathrm{m}^2/\mathrm{s}$.

In RC-regime $F_s(\mathbf{q},t)$ is involved in the time dependence of scattering intensity in a more complicated way. However, the sensitivity of the time dependences to diffusive motion of atoms in the sample is quite strong. The diffusion causes a drastic transformation of the dynaimical beat structure. The RC regime extends the sensitivity of the method to diffusion coefficient up to $D<10^{-13}\,\mathrm{m}^2/\mathrm{s}$. This method may have some advantages, for instance, the instrumental vibrations which might be due to the resonator motion in QB-regime are absent excluding a possible hide of low velocity diffusion motion.

ACKNOWLEDGMENTS

The support of this work was partially provided by INTAS-RFBR under Contract No. 95-0586. GVS is grateful that DAAD granted his stay in Germany.

*Also at Physik Department E-13, Technische Universität München, D-85748 Garching, Germany.

[1] D. A. O'Connor and N. M. Butt, Phys. Lett. **7**, 233 (1963).
[2] D. C. Champaney, Rep. Prog. Phys. **42**, 1017 (1979).
[3] Yu. F. Krupyanskii, V. I. Goldanskii, G. U. Nienhaus, and F. Parak, Hyperfine Interact. **53**, 59 (1990).
[4] A. Q. R. Baron, H. Franz, A. Meyer, R. Rüffer, A. I. Chumakov, E. Burkel, and W. Petry, Phys. Rev. Lett. **79**, 2823 (1997).
[5] K. Ruebenbauer and U. D. Wdowik, Phys. Rev. B **58**, 11 896 (1998).
[6] B. Sepiol, M. Kaisermayer, H. Thiess, G. Vogl, E. E. Alp, and W. Sturhahn, Hyperfine Interact. **126**, 329 (2000).
[7] Z. G. Pinsker, *Dynamical Scattering of X-rays in Crystal* (Springer, Heidelberg, 1984).
[8] Yu. Kagan, A. M. Afanas'ev, and V. G. Kohn, J. Phys. C **12**, 615 (1979).
[9] V. G. Kohn and Yu. V. Shvyd'ko, J. Phys.: Condens. Matter **7**, 7589 (1995).
[10] G. V. Smirnov and V. G. Kohn, Phys. Rev. B **52**, 3356 (1995).
[11] G. V. Smirnov, Hyperfine Interact. **97/98**, 552 (1996).
[12] V. G. Kohn and G. V. Smirnov, Phys. Rev. B **57**, 5788 (1998).
[13] G. V. Smirnov, Hyperfine Interact. **123/124**, 31 (1999).
[14] L. Van Hove, Phys. Rev. **95**, 249 (1954).
[15] K. S. Singwi and A. Sjölander, Phys. Rev. **120**, 1093 (1960).